SHORT COMMUNICATIONS

Acta Cryst. (1996). B**52**, 892–895

The *ab initio* crystal structure determination of vapour-deposited methyl fluoride by high-resolution neutron powder diffraction

R. M. IBBERSON[a]* AND M. PRAGER[b] *at* [a]*ISIS Facility, Rutherford Appleton Laboratory, Chilton, Didcot, Oxfordshire OX11 0QX, England, and* [b]*Institut für Festköperforschung der KFA Jülich Postfach 1913, W5170 Jülich, Germany.*
E-mail: rmi@isise.rl.ac.uk

(*Received 28 March 1996; accepted 8 May 1996*)

Abstract

The crystal structure of methyl fluoride (m.p. = 131 K, b.p. = 195 K) at 5 K has been solved *ab initio* from high-resolution neutron powder diffraction data. A good quality powder sample was produced using a vapour deposition technique and enabled an accurate and precise structure refinement to be carried out; the C—F bond length is 1.399 (4) Å and the average C—D bond length is 1.070 (4) Å. The monoclinic structure may be described in terms of dipole–dipole intermolecular interactions and is distinct from the structures of the other methyl halides.

1. Introduction

The methyl halides, CH_3X, represent some of the simplest polar molecular solids and, therefore, not surprisingly, have been intensively studied in recent years by a variety of spectroscopic techniques (see review by Anderson, Andrews & Torrie, 1985). These simple molecular crystals can be used to derive hydrogen–halide interatomic pair potentials by describing consistently the lattice dynamics and rotational tunnelling (Prager, 1988), provided the crystal structure is accurately known.

In the case of X = I, Br, Cl, the spectroscopic data can be reliably interpreted on the basis of known low-temperature crystal structures. The known methyl halide crystal structures are closely related. The structures of CH_3I (Kawaguchi *et al.*, 1973) and the low-temperature β-phase of CH_3Br (Kawaguchi *et al.*, 1973; Gerlach, Torrie & Powell, 1986) are orthorhombic, space group *Pnma*. The chloride structure (Burbank, 1953) and bromide high-temperature α-phase structure (Gerlach, Torrie & Powell, 1986) corresponds to the orthorhombic space group $Cmc2_1$. Both structures may be described in terms of a quasi-two-dimensional motif defined by C—H$\cdots X$ bonds. In the α-phase structure these layers of molecules are aligned head-to-head, whereas in the β-phase structure there is an inversion of every second molecule resulting in a head-to-tail sequence within each layer.

The crystal structure of CH_3F was previously unknown. However, a number of inferences have been made from spectroscopic data. Systematic behaviour observed in the crystal structure studies of the methyl halides naturally led to the interpretation of spectroscopic data on CH_3F following these assumptions; for example, Reynhardt, Pratt & Watton (1986), NMR; Chao & Eggers (1977), IR and Raman. On the other hand, inelastic incoherent neutron spectroscopy (Prager, 1988) shows that the systematic increase of rotational potentials breaks down with CH_3F. This indicates that the crystal structure is fundamentally different. Low-temperature Raman and IR spectra (Binbrek, Anderson & Torrie, 1985) also report a different structure from the known methyl halides, implying a primitive centrosymmetric structure with at least eight molecules in the unit cell. Clearly, for the correct interpretation of spectroscopic data it is very important to solve the crystal structure. Of further interest is a recent ambient-temperature high-pressure Raman study (Wu & Shimizu, 1995), which reports an orientationally disordered phase of CH_3F above 2.75 GPa, reminiscent of CF_4, which transforms to an orientationally ordered phase above 3.63 GPa.

The low melting points and low boiling points of the methyl halides present particular difficulties for crystal structure investigations; all are gases under ambient conditions, apart from CH_3I which is a liquid. In spite of this, single-crystal studies have been carried out on CH_3Cl (Burbank, 1953), CH_3Br and CH_3I (Kawaguchi *et al.*, 1973). However, CH_3F, with a much lower melting point of 131 K and boiling point of 195 K, presents severe technical difficulties for single crystal growth and subsequent diffraction studies. Under these circumstances the technique of powder diffraction, particularly at high resolution, is known to provide a useful alternative for structure refinement (David & Ibberson, 1992; Ibberson, David & Prager, 1992) and, more recently, *ab initio* structure solution has been found to be possible assuming a good quality powder sample can be produced (Ibberson & Prager, 1995).

2. Experimental

A powder sample of perdeuterated methyl fluoride, CD_3F, supplied by Cambridge Isotope Laboratories (CIL), Massachusetts, USA, was produced using a vapour deposition technique. The sample was prepared in a standard vanadium-tailed liquid-helium orange cryostat using a gas inlet line based on a design by Langel, Kollhoff & Knözinger (1986). The gas is deposited at a controlled low rate (20–60 cm^3 min^{-1} at standard temperature and pressure) in a standard cylindrical vanadium sample tube (diameter 15 mm, height 40 mm). A low rate of deposition is essential in order to keep the heat dissipation during condensation to a minimum and thus prevent the powder from annealing or melting. The vanadium tube has a copper disc at its base (see Fig. 1) and a copper finger is mounted on the disc inside the tube to serve as a cold point within the lower part of the can to initiate condensation of the gas. The inlet line comprises three coaxial stainless steel tubes. The can is connected, *via* an indium seal, to the outer tube of the inlet line and cooled by He exchange gas in the cryostat. The central capillary line, through which the gas is passed, is thermally

isolated from cold points of the cryostat by means of a vacuum to the middle tube and from the sample by the vacuum (low gas pressure) above the sample during condensation conditions. The capillary may be heated using thermo-coaxial wires and the temperature gradient along the inlet line monitored using type-K NiCr–Ni thermocouples. The temperature is also monitored using RhFe sensors mounted at the base of the can and at the heat exchanger inside the cryostat.

The temperature at which vapour deposition occurs greatly affects the quality of the powder sample produced. Preferred orientation is to be avoided if at all possible, however, line broadening due to strain and particle size effects in the powder sample must also be considered. Condensation close to the melting point typically produces a less strained sample, but can produce large crystallites and give rise to preferred orientation effects, especially if recrystallization occurs. The converse is true for condensation temperatures well below the melting point. The difference between condensing and annealing a sample at a given temperature should also be noted. The sample becomes more polycrystalline when condensing rather than annealing at a given temperature since, with the former, any reconstruction requires mobility only at a two-dimensional surface, which occurs easier than in the three-dimensional bulk sample necessary in the latter case. Finally, a high vapour pressure of methyl fluoride could make a thermal short-circuit to the warm nozzle and hinder a controlled condensation. This was also an important factor in selecting an appropriate deposition temperature. The final sample of some 3 cm^3 was condensed at 80 K ($\sim 0.6 \times T_{mp}$; negligible vapour pressure of CD_3F) over a period of some 2 h.

Time-of-flight neutron powder diffraction data were collected on the high-resolution powder diffractometer, HRPD (Ibberson, David & Knight, 1992), at the ISIS pulsed neutron source. A time-of-flight diffractometer such as HRPD utilizes a polychromatic neutron beam and, therefore, data are recorded by fixed-angle detectors. Neutron wavelengths are discriminated by their time of arrival since $t \propto 1/v_n \propto \lambda_n \propto d$, where t is the time of flight, v_n is the neutron velocity, λ_n is the neutron wavelength and d is the d-spacing of a particular Bragg reflection. For the present experiments at backscattering ($< 2\theta > = 168°$) and 90°, the time-of-flight range used was 20–120 ms, corresponding to a total d-spacing range of ~ 0.4–3.4 Å. Under these experimental settings the diffraction data have an approximately constant resolution of $\Delta d/d = 8 \times 10^{-4}$ at backscattering and $\Delta d/d = 5 \times 10^{-3}$ at 90°.

Diffraction data were recorded at 5 and 80 K, each for a period of some 12 h. No evidence for structural phase transitions was observed. No evidence of preferred orientation was observed following tests monitoring intensity variations of strong reflections on rotation of the sample around the vertical axis.

A standard data reduction procedure was followed: the data were normalized to the incident beam monitor profile and corrected for detector efficiency effects using a previously recorded vanadium spectrum.

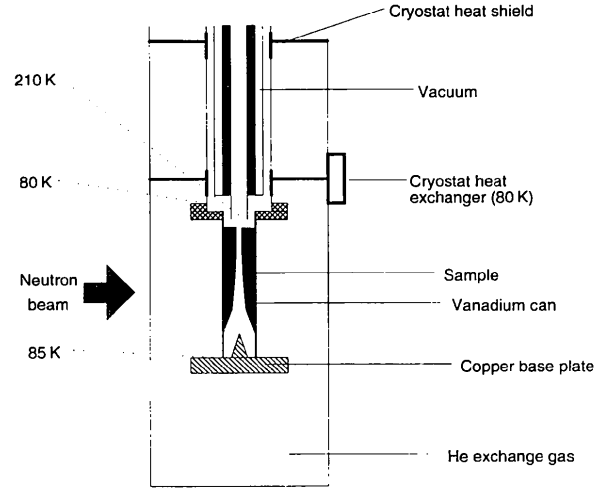

Fig. 1. Schematic drawing of the experimental set-up for vapour deposition (temperatures shown correspond to those during sample preparation by vapour deposition).

3. Structure solution and refinement

The efficacy of the sample preparation allowed structure solution and refinement to be carried out routinely using the high-resolution neutron powder data. The first 20 low-order Bragg reflections at 5 K were located by visual inspection, to an accuracy of 0.001 Å, with determination of the unit-cell carried out using the autoindexing program *ITO* (Visser, 1988). A monoclinic cell was determined, $V_c = 186.73$ $Å^3$, with a figure of merit $M(20)$ of 28.2 and no unindexed lines.

The highest symmetry space group consistent with the systematic absences is $P2_1/n$. In agreement with the results of inelastic neutron scattering experiments (Prager, 1988), the structure comprises one molecule on a general position in the asymmetric unit, thus all methyl groups are crystallographically equivalent.

Structure-factor amplitudes were extracted using a Bayesian approach formulated by Sivia & David (1994) and fully described elsewhere (Ibberson & Prager, 1995). Reliable intensity information could be extracted for a total of 337 structure-factor amplitudes, $|F(hkl)|$, to a minimum d-spacing of 0.832 Å, which were used as input to the direct-methods program *MITHRIL* (Gilmore, 1983). The program was run using default parameters. After normalization, 120 of the

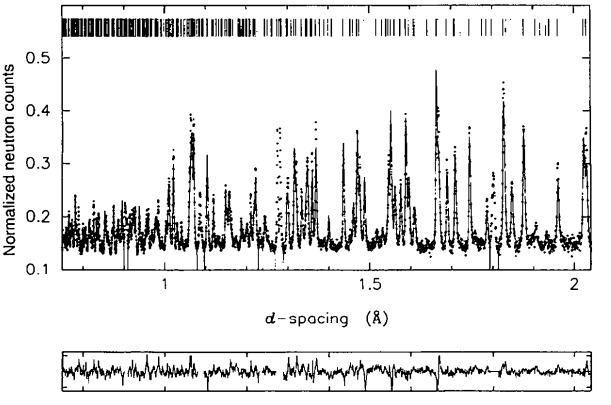

Fig. 2. Observed (dots) and calculated (line) powder diffraction profiles for CD_3F at 5 K. The vertical tick marks are the calculated positions of Bragg peaks, excluded regions correspond to the positions of Cu Bragg peaks. The lower trace corresponds to the difference profile divided by the e.s.d. of each point; dotted lines correspond to $\pm 3\sigma$.

Table 1. *Refined structural parameters for CD_3F at 5 K*

Monoclinic: Space group $P2_1/n$ (no. 14).
Lattice constants: $a = 6.4373(1)$, $b = 7.5023(1)$, $c = 3.9598(2)$ Å, $\beta = 101.842(1)°$ [80 K: $a = 6.5021(2)$, $b = 7.5369(1)$ $c = 3.9840(3)$ Å, $\beta = 101.613(2)°$].
Volume per molecule: 46.79 Å^3 (80 K: 47.81 Å^3).
Calculated density: 1.313 g cm^{-3} (80 K: 1.286 g cm^{-3}).

	x	y	z	U_{iso} (Å^2)
C	0.7310 (4)	0.1501 (1)	0.8553 (7)	0.009 (1)
F	0.6923 (4)	0.3103 (3)	1.0125 (6)	0.002 (1)
D(1)	0.8495 (6)	0.1714 (5)	0.7024 (8)	0.024 (1)
D(2)	0.5876 (6)	0.0987 (6)	0.7026 (9)	0.036 (1)
D(3)	0.7914 (6)	0.0594 (4)	1.0590 (7)	0.019 (1)

$R_o = 4.98\%$, $R_{wP} = 6.39\%$, $R_E = 2.91\%$, $\chi^2 = 4.81$ for 3583 and 43 basic variables.

Table 2. *Intra- and intermolecular bond lengths (Å) and angles (°)*

(*a*) Intramolecular

C—F	1.399 (4)	C—D(2)	1.066 (5)
C—D(1)	1.079 (4)	C—D(3)	1.066 (4)
F—C—D(1)	109.5 (3)	D(1)—C—D(2)	111.4 (4)
F—C—D(2)	110.5 (4)	D(2)—C—D(3)	109.7 (4)
F—C—D(3)	106.4 (3)	D(1)—C—D(3)	109.3 (4)

(*b*) Shortest intermolecular distances

	Along [101]	Along [010]
D(1)···F	2.477 (5)	2.835 (4)
D(2)···F	2.593 (5)	2.814 (4)
D(3)···F	2.512 (4)	2.990 (4)

observed reflections had $|E|$ values >1.0 and were available for the development of phase relationships. A standard direct methods calculation led to an *E*-map in which the first five peaks, based on relative peak height, were assigned to atoms. Examination of the bond lengths and angles between these peaks permitted an unambiguous assignment of the atoms. The atomic coordinates determined in the direct-methods calculations were subsequently used as a starting model for the full profile refinement of the structure.

The results of the profile fitting (David, Ibberson & Matthewman, 1992) are illustrated in Fig. 2, with the final refined structural and profile parameters listed in Table 1. Anisotropic displacement parameters could not be refined reliably. Selected bond lengths and angles calculated from the refined atomic coordinates are given in Table 2. Regions of the profile containing Bragg peaks from copper and vanadium of the sample environment equipment were excluded from the refinement. To overcome this loss of information, bond lengths and angles within the methyl group were weakly restrained to be equivalent to within ±0.005 Å and ±0.5°, respectively, during the refinement. This method using soft constraints, whilst biasing the fit towards a chemically reasonable result, does not dictate precise bond lengths and angles.

4. Discussion

The monoclinic crystal structure of methyl fluoride (see Fig. 3) contains four molecules in the unit cell and one molecule in the asymmetric unit. The crystal structure is fully consistent with tunnel splitting of the methyl librational ground state observed by inelastic neutron scattering (Prager, 1988) and may well correspond to the ordered phase at 300 K above 2.75 GPa reported from Raman studies (Wu & Shimizu, 1995). No evidence of the plastic phase, recorded during the high-pressure Raman measurements, was observed in the present low-temperature ambient pressure measurements.

Methyl fluoride is a polar molecule with a large permanent dipole moment, $\mu = 1.85$ D (Anderson, Andrews & Torrie, 1985). The effects of dipole–dipole coupling are, therefore, expected to be reflected by structural features and this is found to be the case. The intramolecular C—F bond length clearly shows evidence of bond polarization. The equilibrium value determined by gas-phase electron diffraction is 1.382 Å (Duncan, 1970) compared with 1.399 (4) Å in the present study. The effect is less pronounced in monofluoroacetamide, which has a C—F bond length of 1.3906 (5) Å at 20 K, as determined using single-crystal neutron diffraction (Jeffrey, Ruble, McMullan, DeFrees & Pople, 1981). However, the average C—H bond length in the gas-phase study of 1.095 Å and average H—C—H bond angle of 110.2° compare well with values determined in the present study of 1.070 (4) Å and 110.1 (4)°, respectively.

The structure can be described in terms of zigzag head-to-tail chains of molecules running up and down the *b* axis of the crystal. In this direction the average C—D···F contact is 2.880 (4) Å. The closest C—D···F intermolecular contacts, however, are found essentially in the *ac* plane and primarily along **a** (see Table 2) with two contacts of *ca* 2.5 Å and a third at *ca* 2.6 Å. *Ab initio* molecular orbital calculations on clusters of methyl fluoride have been carried out using the *Gaussian*70 program with the minimal STO-3G and the 4-31G basis sets (Oi, Sekreta & Ishida, 1983). Whilst there is a broad agreement

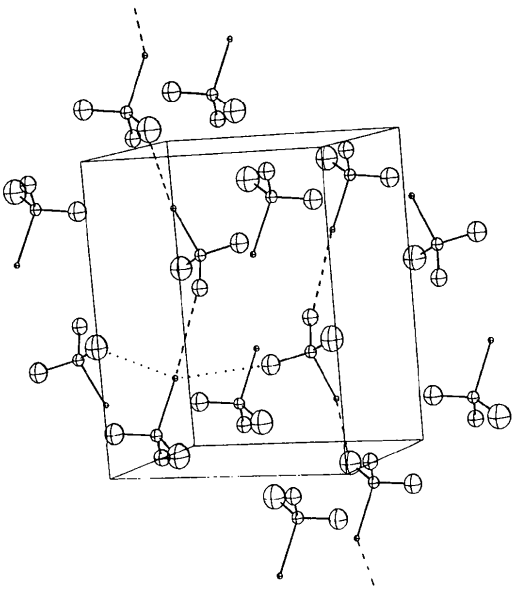

Fig. 3. Schematic illustration, drawn using *ORTEP*II (Johnson, 1971), of the structure of CD_3F at 5 K. Thermal ellipsoids are drawn at the 50% probability level. The shortest intermolecular contacts are indicated by dashed lines along the *b* axis and by dotted lines in the *ac* plane (see Table 2*b*). For reasons of clarity, not all intermolecular distances have been shown.

between dipole orientations in the observed structure and the cluster calculations, the optimum C—D···F configuration in any of the modelled clusters is calculated to be linear and at a much shorter distance of 2.1 Å. This configuration determined by *ab initio* calculations is, therefore, more consistent with the crystal structure of CH_3Cl and also indicative of a stronger C—H···*X* interaction in methyl fluoride than that for methyl chloride (Oi, Sekreta & Ishida, 1983). The weak hydrogen bonds observed in the CD_3F structure may well account for methyl fluoride showing the weakest rotational potential of all methyl halides (Prager, 1988) and the departure from the anticipated systematic structural behaviour.

References

Anderson, A., Andrews, B. & Torrie, B. H. (1985). *J. Chim. Phys.* **82**, 99–109.

Binbrek, O. S., Anderson, A. & Torrie, B. H. (1985). *J. Raman Spectrosc.* **16**, 185–189.

Burbank, R. D. (1953). *J. Am. Chem. Soc.* **75**, 1211–1214.

Chao, T. H. & Eggers, D. F. (1977). *J. Chem. Phys.* **66**, 970–975.

David, W. I. F. & Ibberson, R. M. (1992). *Acta Cryst.* C**48**, 301–303.

David, W. I. F., Ibberson, R. M. & Matthewman, J. C. (1992). Rutherford Appleton Laboratory Report, RAL-92-032.

Duncan, J. L. (1970). *J. Mol. Struct.* **6**, 447–457.

Gerlach, P. N., Torrie, B. H. & Powell, B. M. (1986). *Mol. Phys.* **57**, 919–930.

Gilmore, C. J. (1983). *MITHRIL. A Computer Program for the Automatic Solution of Crystal Structures from X-ray Data.* Version 1.0. Department of Chemistry, University of Glasgow, Glasgow G12 8QQ, Scotland.

Ibberson, R. M. & Prager, M. (1995). *Acta Cryst.* B**51**, 71–76.

Ibberson, R. M., David, W. I. F. & Knight, K. S. (1992). Rutherford Appleton Laboratory Report, RAL-92-031.

Ibberson, R. M., David, W. I. F. & Prager, M. (1992). *J. Chem. Soc. Chem. Commun.* pp. 1438–1439.

Jeffrey, G. A., Ruble, J. R., McMullan, R. K., DeFrees, D. J. & Pople, J. A. (1981). *Acta Cryst.* B**37**, 1885–1890.

Johnson, C. K. (1971). *ORTEP*II. Report ORNL-3794. Oak Ridge National Laboratory, Tennessee, USA.

Kawaguchi, T. K., Hijikigawa, M., Hayafuji, Y., Ikeda, M., Fukushima, R. & Tomie, Y. (1973). *Bull. Chem. Soc. Jpn*, **46**, 53–56.

Langel, W., Kollhoff, H. & Knözinger, E. (1986). *J. Phys. E*, **19**, 86–87.

Oi, T., Sekreta, E. & Ishida, T. (1983). *J. Phys. Chem.* **87**, 2323–2329.

Prager, M. (1988). *J. Chem. Phys.* **89**, 1181–1184.

Reynhardt, E. C., Pratt, J. C. & Watton, A. (1986). *J. Phys. C*, **19**, 919–928.

Sivia, D. S. & David, W. I. F. (1994). *Acta Cryst.* A**50**, 703–714.

Visser, J. W. *Sci. Instrum Sci. Instrum Sci. Instrum* (1988). *ITO. Autoindexing Program.* Technisch Physische Dienst, PO Box 155, Delft, The Netherlands.

Wu, Y. H. & Shimizu, H. (1995). *J. Chem. Phys.* **102**, 1157–1163.